Journal of Simulation & Analysis of Novel Technologies in Mechanical Engineering
10 (3) (2017) 0005~0018
HTTP://JSME.IAUKHSH.AC.IR
ISSN: 2008-4927

Dynamic Instability Analysis of Embedded Multi-walled Carbon Nanotubes under Combined Static and Periodic Axial Loads using Floquet-Lyapunov Theory

Habib Ramezannejad Azarboni[1,*], Hemad Keshavarzpour[2], Reza Ansari[3]

1- Department of Mechanical Engineering, Ramsar branch, Islamic Azad University, Ramsar, Iran.

2- Department of Mechanical Engineering, Rasht branch, Islamic Azad University, Rasht, Iran.

3- Department of Mechanical Engineering, Guilan University, Rasht, Iran

**Corresponding Author: h.ramezannejad@iaukhsh.ac.ir*

(Manuscript Received --- 06, 2017; Revised --- 10, 2017; Accepted --- 11, 2017; Online --- 11, 2017)

Abstract

The dynamic instability of single-walled carbon nanotubes (SWCNT), double-walled carbon nanotubes (DWCNT) and triple-walled carbon nanotubes (TWCNT) embedded in an elastic medium under combined static and periodic axial loads are investigated using Floquet–Lyapunov theory. An elastic multiple-beam model is utilized where the nested slender nanotubes are coupled with each other through the van der Waals (vdW) interlayer interaction. Moreover, a radius-dependent vdW interaction coefficient accounting for the contribution of the vdW interactions between adjacent and non-adjacent layers is considered. The Galerkin's approximate method on the basis of trigonometric mode shape functions is used to reduce the coupled governing partial differential equations to a system of extended Mathieu-Hill equations. Applying Floquet–Lyapunov theory, the effects of elastic medium, length, number of layers and exciting frequencies on the instability conditions of CNTs are investigated. Results show that elastic medium, length of CNTs, number of layer and exciting frequency have significant effect on instability conditions of multi-walled CNTs.

Keywords: Dynamic instability, multi-walled carbon nanotubes, Mathieu-Hill model, Floquet-Lyapunov theory.

1- Introduction

The excellent physical (e.g. mechanical, thermal and electrical) and chemical properties, and the low density of carbon nanotubes (CNTs), make these novel nanostructured materials very promising for advanced applications. Theoretical methods for modeling of CNTs can be classified into atomistic approaches, including classical molecular dynamics, density functional theory and tight-binding molecular dynamics, as well as continuum mechanics approaches including beam models, shell models and space frame models. Vibration, bending, stress analysis, buckling and instability analysis of CNTs have been of interest to numerous researchers from different disciplines. Based on different theoretical modeling, the static and dynamic instability analysis

of CNTs have been investigated under bending, axial and torsional loading to predict the instability conditions. Considering the effects of surrounding elastic medium and van der Waals forces and based on the continuum modeling, bending instability and bifurcation conditions of an embedded double-walled carbon nanotube were investigated by Han et al. [1].

Yoon et al. [2] studied the influence of internal moving fluid on structural instability and free vibration of single-walled carbon nanotubes conveying fluid by employing the classic Euler-beam model. They investigated the effect of internal moving fluid on flutter instability of cantilever carbon nanotubes as well as free vibration of cantilever single-walled carbon nanotubes [3]. They concluded that stiffness of elastic medium has a significant effect on elimination of flow-induced flutter instability. Using of Raman spectroscopy and documented by TEM imaging, Hadjiev et al. [4] carried out analysis of buckling instabilities of octadecylamine functionalized single-walled carbon nanotubes embedded in epoxy. Based on continuum-atomistic (CA) approach, investigation of single-walled CNTs were examined out by Volokh and Ramesh [5] to analyze the tensile instability and bifurcation conditions. Tylikowski [6] studied the dynamic instability of CNTs using continuum mechanics along with an elastic layered shell model and considering thermal effects. Wang et al. [7] investigated the instability of single-walled zigzag and armchair carbon nanotubes by using of a hybrid continuum and molecular mechanics model. By means of continuum elastic-beam model and differential quadrature method, the instability conditions of single-walled CNTs were investigated by Wang and Ni [8]. Wang et al. [9] investigated the natural vibrations and buckling instability of double-wall carbon nanotubes (DWNTs) conveying fluid using a multi-elastic beam model and considering intertube radial displacements along with their related internal degrees of freedom. By molecular dynamics approach, Wang [10] carried out the torsional instability analysis of a single-walled carbon nanotube containing C60 fullerenes.

The nonlinear dynamic instability analysis of double-walled nanotubes was numerically investigated by Fu et al. [11] by employing the multiple-elastic beam model based on Euler-Bernoulli-beam theory. The vibration and instability analysis of single-walled CNTs conveying fluid embedded in a linear viscoelastic medium based on the classical Euler–Bernoulli beam model were investigated by Ghavanloo et al. [12]. Ghavanloo and Fazelzadeh [13] investigated the Flow-thermoelastic vibration and instability analysis of viscoelastic CNTs embedded viscos fluid by using of nonlocal Timoshenko beam model. In this investigation the effects of structural damping of the CNTs, internal moving fluid, external viscous fluid, temperature change and nonlocal parameter were considered to develop governing equations of CNTs. Natsuki et al. [14] investigated the torsional elastic instability analysis of double-walled CNTs embedded in an elastic medium by employing the continuum elastic shell model and Winkler spring model theoretically. Based on the modified couple stress theory and the Timoshenko beam theory, the vibration and instability of embedded double-walled CNTs conveying fluid were studied by Ke

and Wang [16]. Chang and Liu [17] carried out the instability and bifurcation conditions of double-walled CNTs conveying fluid based on nonlocal elasticity theory and using an elastic shell model based on Donnell's shell theory. Using an elastic shell model based on Donnell's shell theory and nonlocal elasticity theory, the instability of double-walled CNTs conveying fluid were studied by Chang and Liu [18]. Using the thermal elasticity theory and the nonlocal Euler-Bernoulli beam model, the thermal–mechanical vibration and instability analysis of double-walled CNTs conveying fluid embedded in biological soft tissue as a kind of visco-elastic foundation were carried out by Zhen et al. [19]. Shi et al. [20] studied the buckling instability of CNTs based on the nonlocal Euler-Bernoulli beam model and the Whitney–Riley model. Kazemi-Lari et al [21] investigated the instability of cantilever CNTs embedded in a linear viscoelastic medium based on the nonlocal Euler–Bernoulli theory. Static and dynamic instability of fluid-conveying CNTs based on thin-walled beams model was investigated by Choi et al. [22]. Ghorbanpour Arani et al. [23] investigated the vibration and instability of double-walled CNTs conveying fluid embedded in viscoelastic medium based on Timoshenko beam theory. Fakhrabadi et al. [24] studied the instability of electrostatically actuated carbon nanotubes by considering the classical and nonlocal elasticity theory. Considering the nonlocal continuum theory, the dynamical parametric instability of CNTs subjected to axial harmonic excitation was investigated by Wang and Li [25] using Bolotin's method. The dynamic stability analysis of multi-walled CNTs based on effective model and Donnell-shell theory was analytically investigated by Wang et al. [26]. The modified couple stress theory, a material length scale parameter for beam model, the Von Kármán type geometric nonlinearity, the electromechanical coupling and charge equation were considered to derive the nonlinear governing equation. Agha-Davoudi and Hashemian investigated the dynamic stability of SWCNT based on Strain gradient theory and nonlocal Euler-Bernouli beam model [27]. Based on the nonlocal Timoshenko beam theory and considering the surface effect, dynamic stability analysis of functionally graded (FG) nanobeams subjected to axial load in thermal environment were investigated by Saffari and Hashemian [28].

Based on this literature review, the investigation of dynamic instability of CNTs has been limited to the instability analysis of single-walled and double-walled CNTs in which the interaction between non-adjacent layers has not been investigated for DWCNT model. The present work is undertaken with an objective of investigating further the instability analysis of single-walled, double-walled and triple-walled CNTs embedded in an elastic medium under combined static and periodic axial loading by employing Floquet–Lyapunov theory. Moreover, a radius-dependent vdW interaction coefficient accounting for the contribution of the vdW interactions between adjacent and non-adjacent layers is considered. An elastic Bernoulli–Euler beam model, from the view point of continuum mechanics is developed to derive the coupled equations of motion. In order to solve the dynamic governing equations of CNTs, Galerkin's approximate method together with

trigonometric mode shape functions are applied to reduce the coupled governing partial differential equations to a system of the extended Mathieu-Hill equations. The influences of elastic medium, length of CNTs, number of layer and exciting frequency are studied to analysis of stability states of multi-walled CNTs embedded in elastic medium. Results show that elastic medium, length of CNTs, number of layer and exciting frequency have significant effect on instability conditions of multi-walled CNTs.

2- Governing equations

Consider a multi-walled CNT of length *l*, Young's modulus *E*, density ρ, cross-sectional area *A*, and cross-sectional moment of inertia *I*, embedded in an elastic medium. The time-varying displacement components of the nanotube in the *x*, y and *z* directions, as indicated in Fig. 1, are assumed to be (x,t), $v(x,t)$ and $w(x,t)$, respectively.

According to the Bernoulli-Euler beam theory, the equation of motion of a CNT subjected to axial load is:

$$EI\frac{\partial^4 w(x,t)}{\partial x^4} + F(t)\frac{\partial^2 w(x,t)}{\partial x^2} + \rho A\frac{\partial^2 w(x,t)}{\partial t^2} = P(x,t) \quad (1)$$

where $P(x,t)$ can be the pressure exerted on the tube through the vdW interaction forces and/or the interaction between the tube and the surrounding elastic medium, described by the Winkler model and $F(t)$ is the axial load. To capture the effects of the interlayer vdW interactions of all layers in a MWCNTs and to bring the curvature dependence of the vdW interactions into focus, the He's vdW model is employed.

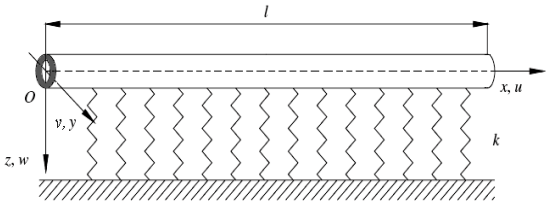

Fig 1. Schematic of a multiwalled CNT embedded in an elastic medium.

$$P(x,t) = \sum_{i=1}^{N} C_{ij}(w_i - w_j) \quad (2)$$

where

$$c_{ij} = \left[\frac{1001\pi\varepsilon\sigma^{12}}{3a^4}E_{ij}^{13} - \frac{1120\pi\varepsilon\sigma^{6}}{9a^4}E_{ij}^{7}\right]R_j \quad (3)$$

here c_{ij} represents the vdW coefficients, $a = 1.42$ Å is the C-C bond length, R_j is the radius of *j*th layer and E_{ij}^{m} with *m* as an integer denotes the elliptic integral defined as:

$$E_{ij}^{m} = \left(R_j + R_i\right)^{-m} \times \int_0^{\frac{\pi}{2}} \left[1 - \frac{4R_jR_i}{\left(R_j + R_i\right)^2}cos^2\theta\right]^{-\frac{m}{2}} d\theta \quad (4)$$

In (1), for the outermost layer which is in contact with the surrounding elastic medium $P(x,t)$ can be described as:

$$P(x,t) = -kw \quad (5)$$

and the axial force is considered to be of the following form

$$F(t) = f_0 + f_1\cos\Omega t \quad (6)$$

Applying (1) to each of the nested tubes along with (2) through (5), the dynamic instability of a MWCNTs is governed by the following set of coupled equations

$$\rho A_1\frac{\partial^2 w_1}{\partial t^2} + EI_1\frac{\partial^4 w_1}{\partial x^4} + F(t)\frac{\partial^2 w_1}{\partial x^2} + \sum_{j=1,j\neq 1}^{n} c_{1j}\left(w_1 - w_j\right) = 0$$

.

.

.

$$\rho A_i \frac{\partial^2 w_i}{\partial t^2} + EI_i \frac{\partial^4 w_i}{\partial x^4} + F(t)\frac{\partial^2 w_i}{\partial x^2} + \sum_{j=1,j\neq i}^{n} c_{ij}(w_i - w_j) = 0$$

.

.

.

$$\rho A_n \frac{\partial^2 w_n}{\partial t^2} + EI_n \frac{\partial^4 w_n}{\partial x^4} + F(t)\frac{\partial^2 w_n}{\partial x^2} + \sum_{j=1,j\neq n}^{n} c_{nj}(w_n - w_j) + kw_n = 0 \quad (7)$$

Given that for a CNT with simply supported boundary conditions at both ends, lateral displacement may be considered as $w(x,t) = W(t)\sin(\frac{m\pi x}{l})$, the dynamic equations of a simply-supported embedded MWCNTs with n layers can be written in term of temporal functions $W_i(t)$, as

$$\frac{d^2W_1}{dt^2} + \left(\frac{m^4\pi^4 EI_1}{l^4\rho A_1} + \sum_{j=1,j\neq 1}^{n}\frac{c_{1j}}{\rho A_1} - F(t)\left(\frac{m\pi}{l}\right)^2\right)W_1 - \sum_{j=1,j\neq 1}^{n}\frac{c_{1j}}{\rho A_1}W_j = 0$$

.

.

$$\frac{d^2W_{\mathrm{i}}}{dt^2} + \left(\frac{m^4\pi^4 EI_{\mathrm{i}}}{l^4\rho A_{\mathrm{i}}} + \sum_{j=1,j\neq \mathrm{i}}^{n}\frac{c_{\mathrm{i}j}}{\rho A_{\mathrm{i}}} - F(t)\left(\frac{m\pi}{l}\right)^2\right)W_i - \sum_{j=1,j\neq \mathrm{i}}^{n}\frac{c_{\mathrm{i}j}}{\rho A_{\mathrm{i}}}W_j = 0 \quad (8)$$

.

.

$$\frac{d^2W_{\mathrm{n}}}{dt^2} + \left(\frac{m^4\pi^4 EI_{\mathrm{n}}}{l^4\rho A_n} + \frac{k}{\rho A_{\mathrm{n}}} + \sum_{j=1,j\neq \mathrm{n}}^{n}\frac{c_{\mathrm{n}j}}{\rho A_{\mathrm{n}}} - F(t)\left(\frac{m\pi}{l}\right)^2\right)W_n - \sum_{j=1,j\neq \mathrm{n}}^{n}\frac{c_{\mathrm{n}j}}{\rho A_{\mathrm{n}}}W_j = 0$$

Now, consider the *i*th field equation of (8) as:

$$\frac{d^2W_i}{dt^2} + \left(\frac{m^4\pi^4 EI_{\mathrm{i}}}{l^4\rho A_{\mathrm{i}}} + \frac{k}{\rho A_{\mathrm{n}}}\delta_{ij} + \sum_{j=1,j\neq \mathrm{i}}^{n}\frac{c_{\mathrm{i}j}}{\rho A_{\mathrm{i}}} - F(t)\left(\frac{m\pi}{l}\right)^2\right)W_i - \sum_{j=1,j\neq \mathrm{i}}^{n}\frac{c_{\mathrm{i}j}}{\rho A_{\mathrm{i}}}W_j = 0 \quad (9)$$

It is useful to express (9) in a non-dimensional form by making use of the following parameters:

$$r = \sqrt{\frac{I_1}{A_1}}, a_i = \frac{W_i}{r}, \omega_l = \frac{m^2\pi^2}{l^2}\sqrt{\frac{EI_1}{\rho\mu A_1}},$$

$$\omega_k = \sqrt{\frac{k}{\rho A_1}}, \omega_c^{ij} = \sqrt{\frac{c_{ij}}{\rho A_i}}, \mu_i = \frac{A_1}{A_i}, \gamma_i = \frac{I_1}{I_i}$$

Considering (6), one can write non-dimensional form of (9) in terms of the extended Mathieu-Hill equation as:

$$\ddot{a}_i + (\eta_{ij} - \beta\cos\Omega t)a_i - \lambda_{ij}a_j = 0 \quad (10)$$

where

$$\eta_{ij} = \frac{\mu_i}{\gamma_i} + \mu_i\left(\frac{\omega_k}{\omega_l}\right)^2\delta_{in} + \sum_{j=1,j\neq i}^{n}\left(\frac{\omega_c^{ij}}{\omega_l}\right)^2 - \alpha \quad (11)$$

$$\alpha = f_0\left(\frac{m\pi}{l\omega_l}\right)^2 \quad (12)$$

$$\beta = f_1\left(\frac{m\pi}{l\omega_l}\right)^2 \quad (13)$$

$$\lambda_{ij} = \sum_{j=1,j\neq i}^{n}\left(\frac{\omega_c^{ij}}{\omega_l}\right)^2 \quad (14)$$

3- Floquet-Lyapunov theory for stability analysis

The Floquet-Lyapunov theory is a straightforward method to investigate the properties of solution, without giving a solution. Based upon Floquet-Lyapunov theorem, the instability of a periodic system can be identified by recognizing the state transition matrix over one period [29]. In consequence, characteristics of real parts of the transition matrix eigenvalues can be used as a stability criterion.

Equation (10) may be transformed into a time-variant state equation in form of:

$$\{\dot{\boldsymbol{y}}\} = \{\boldsymbol{\psi}(t,\boldsymbol{y})\} = [\boldsymbol{\Gamma}(t)]\{\boldsymbol{y}\} \tag{15}$$

in which $\{\boldsymbol{y}\} = \{y_1, y_2, y_3, \dots, y_n\}$ is $n \times 1$ state vector, $\{\boldsymbol{\psi}(t,\boldsymbol{y})\}$ is a vector function and $[\boldsymbol{\Gamma}(t)]$ is $n \times n$ transition matrix with period T, i.e., $\boldsymbol{\Gamma}(t) = \boldsymbol{\Gamma}(t+T)$ which is given by

$$[\boldsymbol{\Gamma}(t)] = \begin{bmatrix} 0 & \boldsymbol{I} \\ -\boldsymbol{K} & 0 \end{bmatrix} \tag{16}$$

where I is a unit matrix and $\boldsymbol{K}$ is a matrix whose elements are defined as

$$K_{mn} = \begin{cases} \eta_{ij} - \beta\cos\Omega t & m = n \\ -\lambda_{ij} & m \neq n \end{cases} \tag{17}$$

In order to compute the transition matrix, $[\boldsymbol{\Gamma}(t)]$, a numerical integration procedure can be applied to (15). Based on the fourth order Runge-Kutta numerical integration with Gill coefficients [27], the ith interval takes the form

$$\{\boldsymbol{y}_{i+1}\} = \{\boldsymbol{y}_i\} + \frac{h}{6}\left[\{\boldsymbol{\Lambda}_1\} + 2\left(1-\frac{1}{\sqrt{2}}\right)\{\boldsymbol{\Lambda}_2\} + 2\left(1+\frac{1}{\sqrt{2}}\right)\{\boldsymbol{\Lambda}_3\} + \{\boldsymbol{\Lambda}_4\}\right] \tag{18}$$

where $h = t_{i+1} - t_i$ is the step size and the vectors $\{\boldsymbol{\Lambda}_1\}$ through $\{\boldsymbol{\Lambda}_4\}$ are also defined as follows

$$\{\boldsymbol{\Lambda}_1\} = \{\boldsymbol{\psi}(t_i, \boldsymbol{y_i})\} \tag{19}$$

$$\{\boldsymbol{\Lambda}_2\} = \left\{\boldsymbol{\psi}\left(\left(t_i + \frac{h}{2}\right), \left(\boldsymbol{y_i} + \frac{1}{2}\boldsymbol{\Lambda}_1\right)\right)\right\} \tag{20}$$

$$\{\boldsymbol{\Lambda}_3\} = \left\{\boldsymbol{\psi}\left(\left(t_i + \frac{h}{2}\right), \left(\boldsymbol{y_i} + \left(\frac{1}{\sqrt{2}} - \frac{1}{2}\right)h\boldsymbol{\Lambda}_1 + \left(1 - \frac{1}{\sqrt{2}}\right)h\boldsymbol{\Lambda}_2\right)\right)\right\} \tag{21}$$

$$\{\boldsymbol{\Lambda}_4\} = \left\{\boldsymbol{\psi}\left((t_i + h), \left(\boldsymbol{y_i} - \frac{1}{\sqrt{2}}h\boldsymbol{\Lambda}_2 + \left(1 + \frac{1}{\sqrt{2}}\right)h\boldsymbol{\Lambda}_3\right)\right)\right\} \tag{22}$$

The following expressions can be derived by combining of (15) and (19)-(22).

$$\{\boldsymbol{\Lambda}_1\} = [\boldsymbol{\Pi}_1(t_i)]\{\boldsymbol{y}_i\} \tag{23}$$

$$\{\boldsymbol{\Lambda}_2\} = [\boldsymbol{\Pi}_2(t_i)]\{\boldsymbol{y}_i\} \tag{24}$$

$$\{\boldsymbol{\Lambda}_3\} = [\boldsymbol{\Pi}_3(t_i)]\{\boldsymbol{y}_i\} \tag{25}$$

$$\{\boldsymbol{\Lambda}_4\} = [\boldsymbol{\Pi}_4(t_i)]\{\boldsymbol{y}_i\} \tag{26}$$

where

$$\boldsymbol{\Pi}_1(t_i) = \boldsymbol{\Gamma}(t_i) \tag{27}$$

$$\boldsymbol{\Pi}_2(t_i) = \boldsymbol{\Gamma}\left(t_i + \frac{h}{2}\right)\left(\boldsymbol{I} + \frac{h}{2}\boldsymbol{\Gamma}(t_i)\right) \tag{28}$$

$$\boldsymbol{\Pi}_3(t_i) = \boldsymbol{\Gamma}\left(t_i + \frac{h}{2}\right)\left(\boldsymbol{I} + h\left(-\frac{1}{2} + \frac{1}{\sqrt{2}}\right)\boldsymbol{\Gamma}(t_i) + h\left(1 - \frac{1}{\sqrt{2}}\right)\boldsymbol{\Pi}_2(t_i)\right) \tag{29}$$

$$\boldsymbol{\Pi}_4(t_i) = \boldsymbol{\Gamma}(t_i + h)\left(\boldsymbol{I} + \frac{h}{\sqrt{2}}\boldsymbol{\Pi}_2(t_i) + h\left(1 + \frac{1}{\sqrt{2}}\right)\boldsymbol{\Pi}_3(t_i)\right) \tag{30}$$

Combining (18), (19)-(22) and (27)-(30) also gives

$$\{\boldsymbol{y}_{i+1}\} = [\boldsymbol{\Phi}(t_i)]\{\boldsymbol{y}_i\} \tag{31}$$

where

$$\boldsymbol{\Phi}(t_i) = [\boldsymbol{I}] + \frac{h}{6}\left[\boldsymbol{\Pi}_1(t_i) + 2\left(1 - \frac{1}{\sqrt{2}}\right)\boldsymbol{\Pi}_2(t_i) + 2\left(1 + \frac{1}{\sqrt{2}}\right)\boldsymbol{\Pi}_3(t_i) + \boldsymbol{\Pi}_4(t_i)\right] \tag{32}$$

Using (31) the following expression can be written out

$$\begin{aligned} \{\boldsymbol{y}(t_1)\} &= [\boldsymbol{\Phi}(t_0)]\{\boldsymbol{y}(t_0)\} \\ \{\boldsymbol{y}(t_2)\} &= [\boldsymbol{\Phi}(t_1)]\{\boldsymbol{y}(t_1)\} \end{aligned} \tag{33}$$

$$= [\boldsymbol{\Phi}(t_1)][\boldsymbol{\Phi}(t_0)]\{\boldsymbol{y}(t_0)\}$$

.
.
.

$$\{\boldsymbol{y}(t_n)\} = [\boldsymbol{\Phi}(t_{n-1})]\{\boldsymbol{y}(t_{n-1})\}$$
$$= [\boldsymbol{\Phi}(t_{n-1})][\boldsymbol{\Phi}(t_{n-2})] \dots [\boldsymbol{\Phi}(t_1)]$$
$$[\boldsymbol{\Phi}(t_0)]\{\boldsymbol{y}(t_0)\}$$

Classification for equilibrium position of the autonomous system can be considered as [14]: If both λ_1 and λ_2 (eigenvalue of transition matrix) are real and $\lambda_1\lambda_2 > 0, \lambda_1 \neq \lambda_2$, the equilibrium position is called a node. If both λ_1 and λ_2 are real and $\lambda_1\lambda_2 < 0$, the equilibrium position is called a saddle point. If λ_1 and λ_2 are complex conjugate with nonzero real part the corresponding equilibrium position is called an unstable focus $[\mathrm{Re}(\lambda_1) > 0]$ or a stable focus $[\mathrm{Re}(\lambda_1) < 0]$. An equilibrium position whose eigenvalues have zero real part is called a non-hyperbolic equilibrium position. The stability of a hyperbolic position cannot be determined from the eigenvalues alone

5. Numerical Results and Discussion

At first, the accuracy and validity of the stability analysis using Floquet-Lyapunov theory is compared with a Fourier stability analytic method for Mathieu Equation. The Mathieu Equation can be considered as;

$$\frac{d^2q(t)}{dt^2} + (\delta + \varepsilon cos(2t))q(t) = 0 \qquad (34)$$

The fundamental solution set in the form of Fourier series with cosine and sine terms having the period 2π can be constructed as:

$$q(t) = \sum_{k=1,3,5}^{2n-1} a_k \cos kt + b_k \sin kt \qquad (35)$$

Substituting the above series in the Mathieu Equation and equating the coefficients of $\cos kt$ or $\sin kt$, the following sets of recursive relations for the a_k and b_k, which are

$$\begin{cases} \left(\delta - 1 + \frac{1}{2}\varepsilon\right)a_1 + \frac{1}{2}\varepsilon a_3 = 0 \\ \frac{1}{2}\varepsilon a_{k-2} + (\delta - k^2)a_k + \frac{1}{2}\varepsilon a_{k+2} = 0 \end{cases} \qquad (36)$$

$$\begin{cases} \left(\delta - 1 - \frac{1}{2}\varepsilon\right)b_1 + \frac{1}{2}\varepsilon b_3 = 0 \\ \frac{1}{2}\varepsilon b_{k-2} + (\delta - k^2)b_k + \frac{1}{2}\varepsilon b_{k+2} = 0 \end{cases} \qquad (37)$$

with $k = 3,5,7$ are obtained. In the stability conditions the determinants of the coefficients must be vanished.

$$\begin{vmatrix} \delta - 1 + \frac{1}{2}\varepsilon & \frac{1}{2}\varepsilon & 0 & 0 & 0 \\ \frac{1}{2}\varepsilon & \delta - 9 & \frac{1}{2}\varepsilon & 0 & 0 \\ 0 & \frac{1}{2}\varepsilon & \delta - 25 & \frac{1}{2}\varepsilon & 0 \\ 0 & 0 & \frac{1}{2}\varepsilon & \delta - 49 & \frac{1}{2}\varepsilon \\ 0 & 0 & 0 & \frac{1}{2}\varepsilon & \delta - k^2 \end{vmatrix} = 0 \qquad (38)$$

$$\begin{vmatrix} \delta - 1 - \frac{1}{2}\varepsilon & \frac{1}{2}\varepsilon & 0 & 0 & 0 \\ \frac{1}{2}\varepsilon & \delta - 9 & \frac{1}{2}\varepsilon & 0 & 0 \\ 0 & \frac{1}{2}\varepsilon & \delta - 25 & \frac{1}{2}\varepsilon & 0 \\ 0 & 0 & \frac{1}{2}\varepsilon & \delta - 49 & \frac{1}{2}\varepsilon \\ 0 & 0 & 0 & \frac{1}{2}\varepsilon & \delta - k^2 \end{vmatrix} \qquad (39)$$

$$\begin{vmatrix} 0 & 0 & 0 \\ 0 & 0 & 0 \\ \frac{1}{2}\varepsilon & 0 & 0 \\ \delta-49 & \frac{1}{2}\varepsilon & 0 \\ \frac{1}{2}\varepsilon & \delta-81 & \frac{1}{2}\varepsilon \\ 0 & \frac{1}{2}\varepsilon & \delta-k^2 \end{vmatrix} = 0$$

Also, the fundamental solution set in the form of Fourier series with cosine and sine terms having the period π can be constructed as:

$$y(t) = a_0 + \sum_{k=2,4,6}^{2n} a_k \cos kt + b_k \sin kt \qquad (40)$$

Substituting the above series in the Mathieu Equation and equating the coefficients of $\cos kt$ or $\sin kt$, the following sets of recursive relations for the a_k and b_k, which are

$$\begin{cases} \delta a_2 + \frac{1}{2}\varepsilon a_0 = 0 \\ \varepsilon a_0 + (\delta-4)a_2 + \frac{1}{2}\varepsilon a_4 = 0 \\ \frac{1}{2}\varepsilon a_{k-2} + (\delta-k^2)a_k + \frac{1}{2}\varepsilon a_{k+2} = 0 \end{cases} \qquad (41)$$

$$\begin{cases} (\delta-4)b_2 + \frac{1}{2}\varepsilon b_4 = 0 \\ \frac{1}{2}\varepsilon b_{k-2} + (\delta-k^2)b_k + \frac{1}{2}\varepsilon b_{k+2} = 0 \end{cases} \qquad (42)$$

with $k = 4,6,8$. Like before, the determinants of the coefficients must be vanished.

$$\begin{vmatrix} \delta & \frac{1}{2}\varepsilon & 0 \\ \varepsilon & \delta-4 & \frac{1}{2}\varepsilon \\ 0 & \frac{1}{2}\varepsilon & \delta-16 \\ 0 & 0 & \frac{1}{2}\varepsilon \\ 0 & 0 & 0 \\ 0 & 0 & 0 \end{vmatrix} \qquad (43)$$

$$\begin{vmatrix} 0 & 0 & 0 \\ 0 & 0 & 0 \\ \frac{1}{2}\varepsilon & 0 & 0 \\ \delta-36 & \frac{1}{2}\varepsilon & 0 \\ \frac{1}{2}\varepsilon & \delta-64 & \frac{1}{2}\varepsilon \\ 0 & \frac{1}{2}\varepsilon & \delta-k^2 \end{vmatrix} = 0$$

$$\begin{vmatrix} \delta-4 & \frac{1}{2}\varepsilon & 0 \\ \frac{1}{2}\varepsilon & \delta-16 & \frac{1}{2}\varepsilon \\ 0 & \frac{1}{2}\varepsilon & \delta-36 \\ 0 & 0 & \frac{1}{2}\varepsilon \\ 0 & 0 & 0 \\ 0 & 0 & 0 \end{vmatrix} \qquad (44)$$

$$\begin{vmatrix} 0 & 0 & 0 \\ 0 & 0 & 0 \\ \frac{1}{2}\varepsilon & 0 & 0 \\ \delta-64 & \frac{1}{2}\varepsilon & 0 \\ \frac{1}{2}\varepsilon & \delta-100 & \frac{1}{2}\varepsilon \\ 0 & \frac{1}{2}\varepsilon & \delta-k^2 \end{vmatrix} = 0$$

Applying the Fourier series method the approximated transition values of δ and ε can be determined for stability regions. The stability regions predicted by Fourier series method are compared with corresponding results of the Floquet-Lyapunov theory in the Figure 2. As depicted in this figure one can be observed a satisfactory accuracy between.

The numerical results are analyzed in the following section to study of instability conditions of multi-walled CNTs based on Floquet-Lyapunov theory. The corresponding material and geometric parameters of the MWCNT are the outer radius $r_{out} = 3\,nm$, the thickness $t = 0.34\,nm$, the length $l = 45\,nm$. Also, mass density of CNTs is $\rho = 1300\,Kg/m^3$ with Young's modulus $E = 1.1\,TPa$. Figs. 3-5 depict the stability and instability regions of SWCNT,

DWCNT and TWCNT embedded in elastic medium respectively. In these figures the unshaded and shaded regions are corresponding to the stability and instability regions respectively. Based on the results in Figs. 3-5 one can conclude that increase of the number of layers will result in more stability in the CNTs. Accordingly, the shaded region corresponding to TWCNTs is shown to be greater than of DWCNTs and shaded region corresponding to DWCNTs is shown to be greater than of SWCNTs.

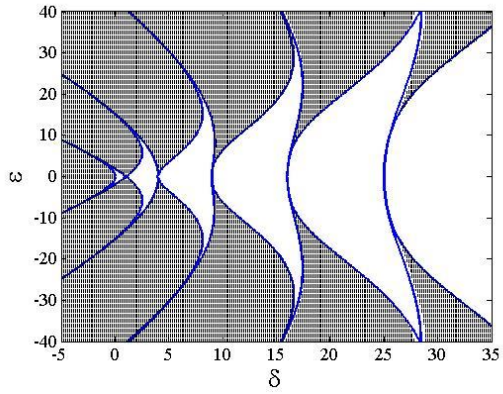

Fig 2. Comparison of Fourier series method's results and the Floquet-Lyapunov theory ones for stability regions of Mathieu Equation

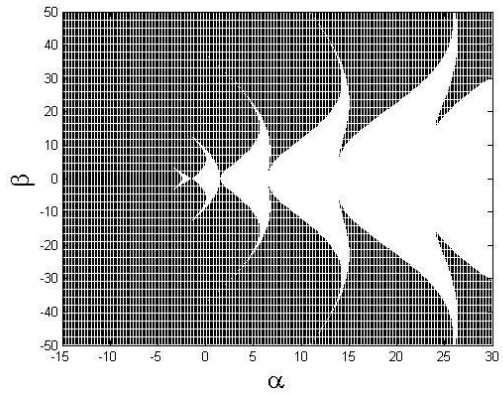

Fig 3. Dynamic instability region of a SWCNT

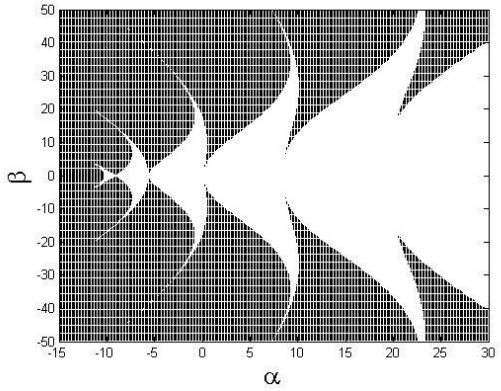

Fig 4. Dynamic instability region of a DWCNT

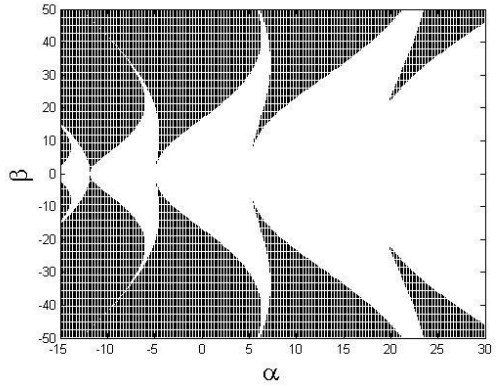

Fig 5. dynamic instability region of a TWCNT

The effect of spring constant of elastic medium at $k = 5 \times 10^8\ N/m^2, k = 0\ N/m^2, k = 5 \times 0^7\ N/m^2,$ and $k = 10^8\ N/m^2$ on the stability and instability regions of triple-walled CNTs under combined static and harmonic axial loading are presented in Figs. 6-9 respectively. As shown, for a specified static load the instability region extends by increasing the dynamic load. Moreover, it is seen that as either the spring constant of elastic medium increases, the stability region grows. In the other word, considering the direct dependence of natural frequency on the constant of elastic medium, one can conclude that the natural frequency has the positive sensitivity on stability conditions of CNTs.

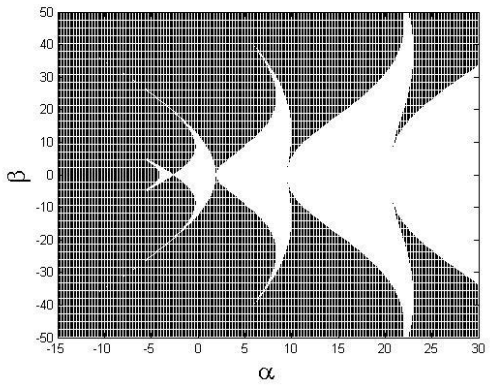

Fig 6. Effect of spring constant on dynamic instability region of a TWCNT $k = 0\ N/m^2$

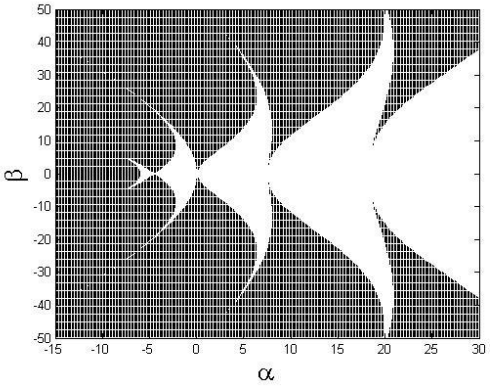

Fig 7. Effect of spring constant on dynamic instability region of a TWCNT $k = 5 \times 10^7\ N/m^2$

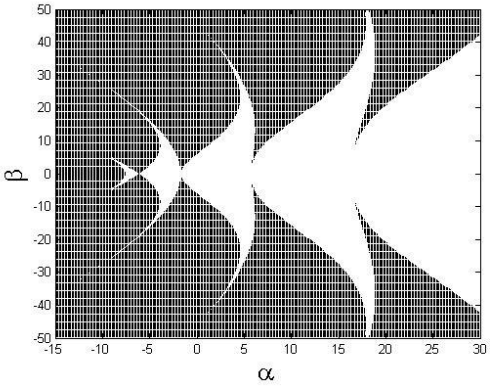

Fig 8. Effect of spring constant on dynamic instability region of a TWCNT $k = 10^8\ N/m^2$

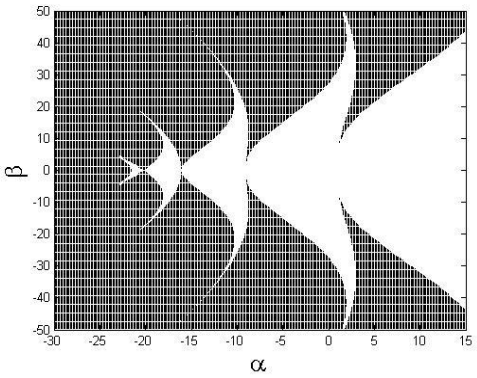

Fig 9. Effect of spring constant on dynamic instability region of a TWCNT $k = 5 \times 10^8\ N/m^2$

The influence of length of triple-walled CNTs at $l = 48\,nm$, $l = 51\,nm$ and $l = 54\,nm$ on unstable region for triple-walled

CNTs are demonstrated in Figs. 8-10 respectively. Comparison between Fig. 4 for $l = 45\,nm$ and Figs. 9-11 for $l = 48\,nm$, $l = 51\,nm$ and $l = 54\,nm$, it can be found that the stability region grows by increasing the length of triple-walled CNTs.

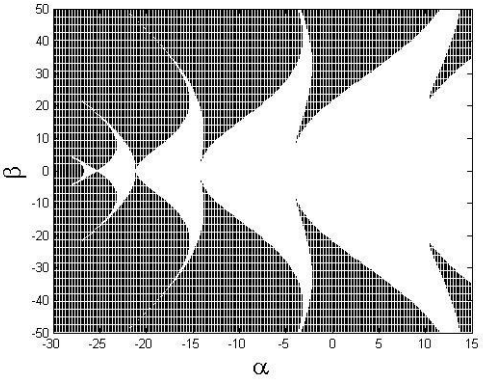

Fig 10. Effect of length on dynamic instability region of a TWCNT $l = 51\ nm$

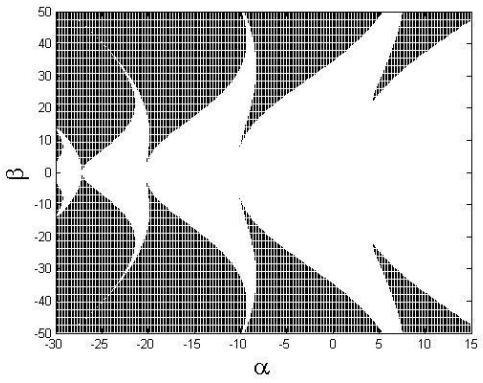

Fig 11. Effect of length on dynamic instability region of a TWCNT $l = 54\ nm$

The effect of exciting frequency at 1 and 3 rad/s on instability of TWCNTs embedded in elastic medium are illustrated in Figs. 12-13, respectively. The elastic constant and length of CNT are considered as $k = 5 \times 10^8\ N/m^2$ and $l = 51nm$. Comparison between Fig. 9 for $\omega = 2\,rad/s$ and Figs. 11-12 for $\omega = 1\,rad/s$ and $\omega = 3\,rad/s$, it can be found that by increasing the exciting frequency the unstable regions shift in static and dynamic load plane.

6. Conclusion

In this study, the dynamic instability of multi-walled carbon nanotubes embedded in elastic medium under combined static and harmonic axial loads using Floquet–Lyapunov theory were investigated. Using the Galerkin's method with trigonometric mode shape functions, reduced to the extended Mathieu-Hill equations.

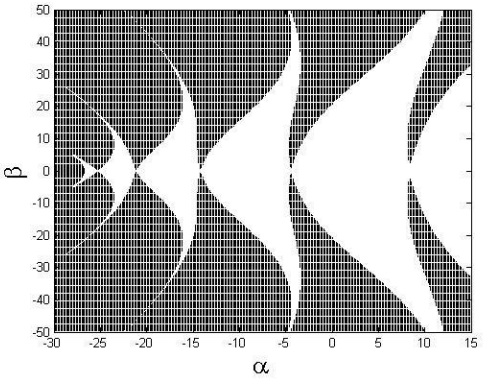

Fig 12. Effect of exciting frequency on dynamic instability region of a triple-walled CNT, $\omega = 1\,rad/s$

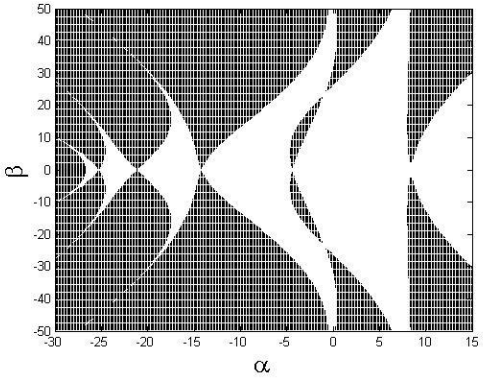

Fig 13. Effect of exciting frequency on dynamic instability region of a triple-walled CNT, $\omega = 3\,rad/s$

The effects of constant of elastic medium, length of multi-walled CNTs, number of layer and exciting frequency were studied on the instability conditions of SWCNTs, DWCNTs and TWCNTs. Remarkable conclusions can be expressed as follows:

1- The Floquet–Lyapunov theory is an efficient numerical method to investigate the dynamic instability of multi-walled CNTs surrounding elastic medium under combined static and periodic loads.
2- The dynamic stability of CNTs increase by increasing the number of layers. For this reason, the TWCNTs is more stable than of DWCNTs and SWCNTs.
3- The dynamic stability response exhibits the positive surrounding elastic medium and length sensitivity of MWCNTs.
4- The dynamic stability response exhibits the negative exciting frequency sensitivity of MWCNTs.
5- By increasing the amplitude of dynamic load parameter the instability region extends for specified amplitude of static load parameter

References

[1] Q. Han, G. Lu, and L. Dai, "Bending instability of an embedded double-walled carbon nanotube based on Winkler and van der Waals models," *Compos. Sci. Technol.*, vol. 65, pp. 1337–1346, 2005.

[2] J. Yoon, C. Q. Ru, and A. Mioduchowski, "Vibration and instability of carbon nanotubes conveying fluid," *Compos. Sci. Technol.*, vol. 65, , pp. 1326–1336, 2005.

[3] J. Yoon, C. Q. Ru, and A. Mioduchowski, "Flow-induced flutter instability of cantilever carbon nanotubes," *Int. J. Solids Struct.*, vol. 43, pp. 3337–3349, 2006.

[4] V. G. Hadjiev *et al.*, "Buckling instabilities of octadecylamine functionalized carbon nanotubes embedded in epoxy," *Compos. Sci. Technol.*, vol. 66, pp. 128–136, 2006.

[5] K. Y. Volokh and K. T. Ramesh, "An approach to multi-body interactions in a continuum-atomistic context: Application to analysis of tension instability in carbon nanotubes," *Int. J. Solids Struct.*, vol. 43, pp. 7609–7627, 2006.

[6] A. Tylikowski, "Instability of thermally induced vibrations of carbon nanotubes," *Arch. Appl. Mech.*, vol. 78, pp. 49–60, Nov. 2007.

[7] Q. Wang, K. M. Liew, and W. H. Duan, "Modeling of the mechanical instability of carbon nanotubes," *Carbon N. Y.*, vol. 46, pp. 285–290, 2008.

[8] L. Wang and Q. Ni, "On vibration and instability of carbon nanotubes conveying fluid," *Comput. Mater. Sci.*, vol. 43, pp. 399–402, Aug. 2008.

[9] L. Wang, Q. Ni, and M. Li, "Buckling instability of double-wall carbon nanotubes conveying fluid," *Comput. Mater. Sci.*, vol. 44, pp. 821–825, 2008.

[10] Q. Wang, "Torsional instability of carbon nanotubes encapsulating C60 fullerenes," *Carbon N. Y.*, vol. 47, pp. 507–512, 2009.

[11] Y. Fu, R. Bi, and P. Zhang, "Nonlinear dynamic instability of double-walled carbon nanotubes under periodic excitation," *Acta Mech. Solida Sin.*, vol. 22, pp. 206–212, 2009.

[12] E. Ghavanloo, F. Daneshmand, and M. Rafiei, "Vibration and instability analysis of carbon nanotubes conveying fluid and resting on a linear viscoelastic Winkler foundation," *Phys. E Low-Dimensional Syst. Nanostructures*, vol. 42, pp. 2218–2224, 2010.

[13] E. Ghavanloo and S. A. Fazelzadeh, "Flow-thermoelastic vibration and instability analysis of viscoelastic carbon nanotubes embedded in viscous fluid," *Phys. E Low-Dimensional Syst. Nanostructures*, vol. 44, pp. 17–24, 2011.

[14] T. Natsuki, T. Tsuchiya, Q. Q. Ni, and M. Endo, "Torsional elastic instability of double-walled carbon nanotubes," *Carbon N. Y.*, vol. 48, pp. 4362–4368, 2010.

[15] W. H. Duan, Q. Wang, Q. Wang, and K. M. Liew, "Modeling the Instability of Carbon Nanotubes: From Continuum Mechanics to Molecular Dynamics," *J. Nanotechnol. Eng. Med.*, vol. 1, pp. 11001, 2010.

[16] L.-L. Ke and Y.-S. Wang, "Flow-induced vibration and instability of embedded double-walled carbon nanotubes based on a modified couple stress theory," *Phys. E Low-dimensional Syst. Nanostructures*, vol. 43, pp. 1031–1039, Mar. 2011.

[17] T.-P. Chang and M.-F. Liu, "Flow-induced instability of double-walled carbon nanotubes based on nonlocal

elasticity theory," *Phys. E Low-dimensional Syst. Nanostructures*, vol. 43, pp. 1419–1426, Jun. 2011.

[18] T.-P. Chang and M.-F. Liu, "Small scale effect on flow-induced instability of double-walled carbon nanotubes," *Eur. J. Mech. - A/Solids*, vol. 30, pp. 992–998, Nov. 2011.

[19] Y. X. Zhen, B. Fang, and Y. Tang, "Thermalmechanical vibration and instability analysis of fluid-conveying double walled carbon nanotubes embedded in visco-elastic medium," *Phys. E Low-Dimensional Syst. Nanostructures*, vol. 44, pp. 379–385, 2011.

[20] J.-X. Shi, T. Natsuki, X.-W. Lei, and Q.-Q. Ni, "Buckling Instability of Carbon Nanotube Atomic Force Microscope Probe Clamped in an Elastic Medium," *J. Nanotechnol. Eng. Med.*, vol. 3, p. 20903, 2012.

[21] M. A. Kazemi-Lari, S. A. Fazelzadeh, and E. Ghavanloo, "Non-conservative instability of cantilever carbon nanotubes resting on viscoelastic foundation," *Phys. E Low-Dimensional Syst Nanostructures*, vol. 44, pp. 1623–1630, 2012.

[22] J. Choi, O. Song, and S.-K. Kim, "Nonlinear stability characteristics of carbon nanotubes conveying fluids," *Acta Mech.*, vol. 224, pp. 1383–1396, 2013.

[23] A. Ghorbanpour Arani, M. R. Bagheri, R. Kolahchi, and Z. Khoddami Maraghi, "Nonlinear vibration and instability of fluid-conveying DWBNNT embedded in a visco-Pasternak medium using modified couple stress theory," *J. Mech. Sci. Technol.*, vol. 27, pp. 2645–2658, Sep. 2013.

[24] M. M. Seyyed Fakhrabadi, A. Rastgoo, and M. Taghi Ahmadian, "Size-dependent instability of carbon nanotubes under electrostatic actuation using nonlocal elasticity," *Int. J. Mech. Sci.*, vol. 80, pp. 144–152, Mar. 2014.

[25] Y.-Z. Wang and F.-M. Li, "Dynamical parametric instability of carbon nanotubes under axial harmonic excitation by nonlocal continuum theory," *J. Phys. Chem. Solids*, vol. 95, pp. 19–23, Aug. 2016.

[26] X. Wang, W. D. Yang, and S. Yang, "Dynamic stability of carbon nanotubes reinforced composites," *Appl. Math. Model.*, vol. 38, pp. 2934–2945, 2014.

[27] F. Agha-Davoudi , M. Hashemian, "Dynamic Stability of Single Walled Carbon Nanotube Based on Nonlocal Strain Gradient Theory" Journal of Solid Mechanics in Engineering, Volume 8, pp 1-11, 2015.

[28] S. Safari , M. Hashemian, "Dynamic Stability of Nano FGM Beam Using Timoshenko Theory" Journal of Solid Mechanics in Engineering, Volume 8, pp 239-250, 2015.

[29] P. Friedman, C. E. Hammond, and T. H. Woo, "Efficient Numerical Treatment of Periodic Systems with Application to Stability Problems," Int. J. Numer. Methods Eng., vol. 11, pp. 1117–1136, 1977.